Supplement Text

S1. Satellite NO_2 retrieval algorithms

The USTC TROPOMI NO_2 product results from the application of satellite NO_2 retrieval algorithms of the GaoFen-5/EMI sensor (Zhang et al., 2020) on TROPOMI. During the NO_2 slant column density retrieval, the wavelength range of 405–465 nm was selected for the NO_2 spectral fit performed with the QDOAS software package[1], following the fit settings by the QA4ECV NO_2 project[2]. Then, the Vector Linearized Discrete Ordinate Radiative-Transfer model[3] was used to calculate the stratospheric and tropospheric NO_2 air mass factor online for each ground pixel. During the radiative transfer calculations, a priori NO_2 profile with a spatial resolution of 20km simulated by WRF-Chem was used[4]. And a Gaussian-weighted reference sector method was applied to separate the stratospheric contribution from the total NO2 column[5,6].

Then, the tropospheric NO_2 VCDs per orbit were re-gridded to the Level 3 product with a resolution of 0.01×0.01 over eastern China by using a novel P-Spline method[7]. Note that satellite pixels were filtered out first if satisfying any of the following rejection criteria: cloud radiance fraction larger than 0.3; root mean square (RMS) of the spectral fitting larger than 0.002; pixels affected by the row anomaly; solar zenith angle larger than 70; and other quality flags[5,7].

S2. Industrial and transport data sources

Data on the cumulative annual increase in the above-scale industry is obtained from the official website of the National Bureau of Statistics of the People's Republic of China (https://data.stats.gov.cn/) and the Hefei Bureau of Statistics (http://tjj.hefei.gov.cn/ydsj/csdbzl/index.html). The industrial production index is based on 2018 and was calculated from the cumulative annual increase in the above-scale industry. Data on road passenger traffic is obtained from the official website of the Ministry of Transport of the People's Republic of China (https://www.mot.gov.cn/tongjishuju/).

Supplement Figures

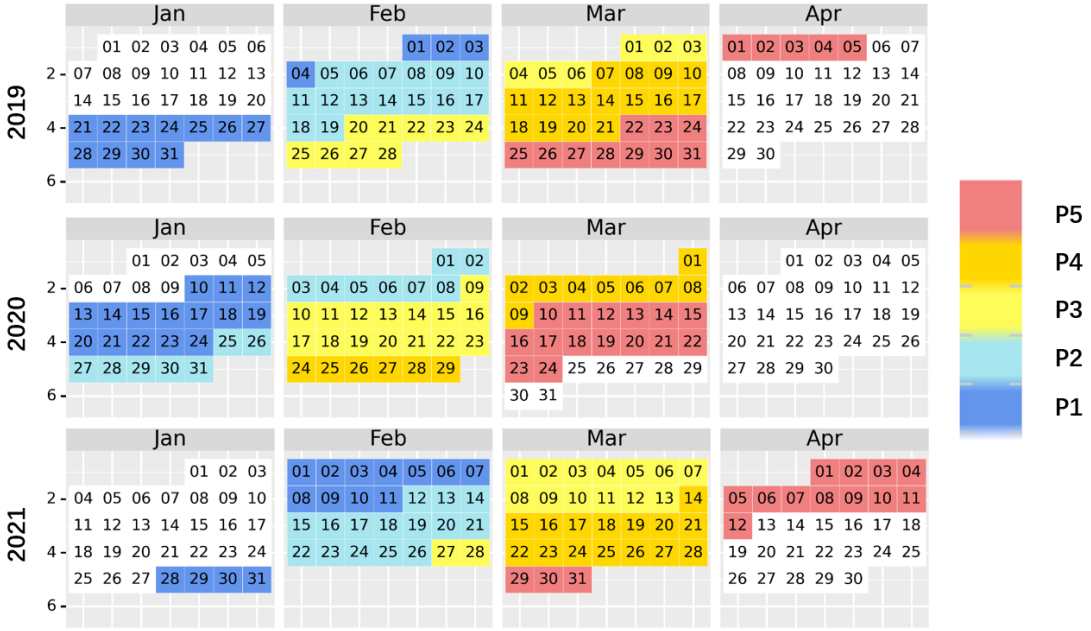


Figure S1. The 5 time phases 2019-2021 divided by Chinese New Year are P1 (15 days before Chinese New Year), P2 (15 days during Chinese New Year), P3 (0 to 15 days after Chinese New Year), P4 (15 to 30 days after Chinese New Year) and P5 (30 to 45 days after Chinese New Year).

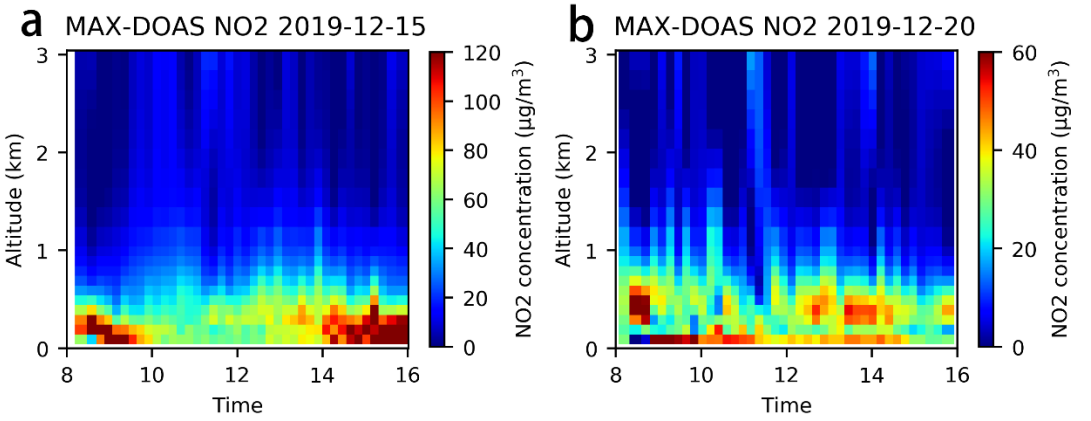


Figure S2. MAX-DOAS NO_2 vertical profile. (a) CAMS site, December 15 2019; (b) CAMS site, December 20 2019.

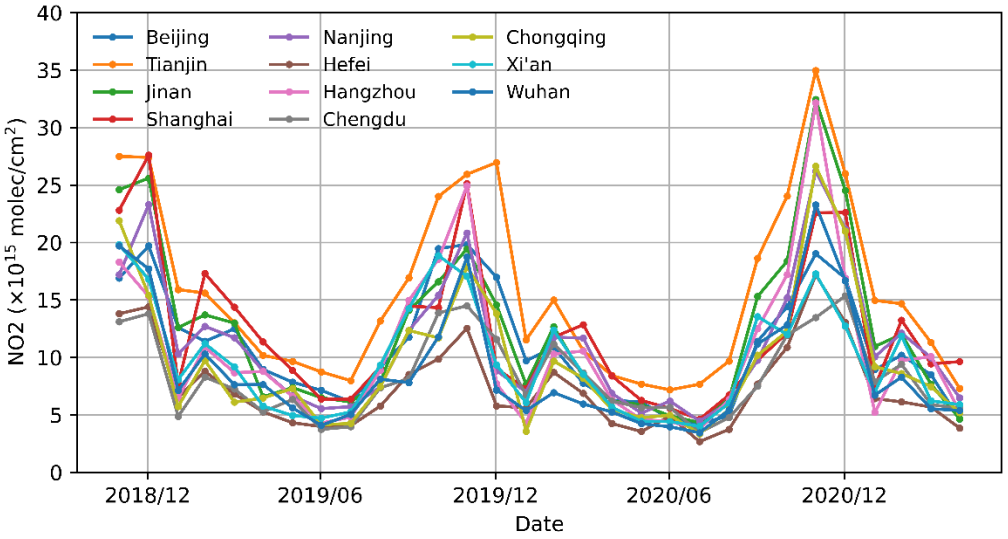


Figure S3. Time series of the monthly mean NO_2 TVCD from December 2018 to May 2021 for selected cities in China.

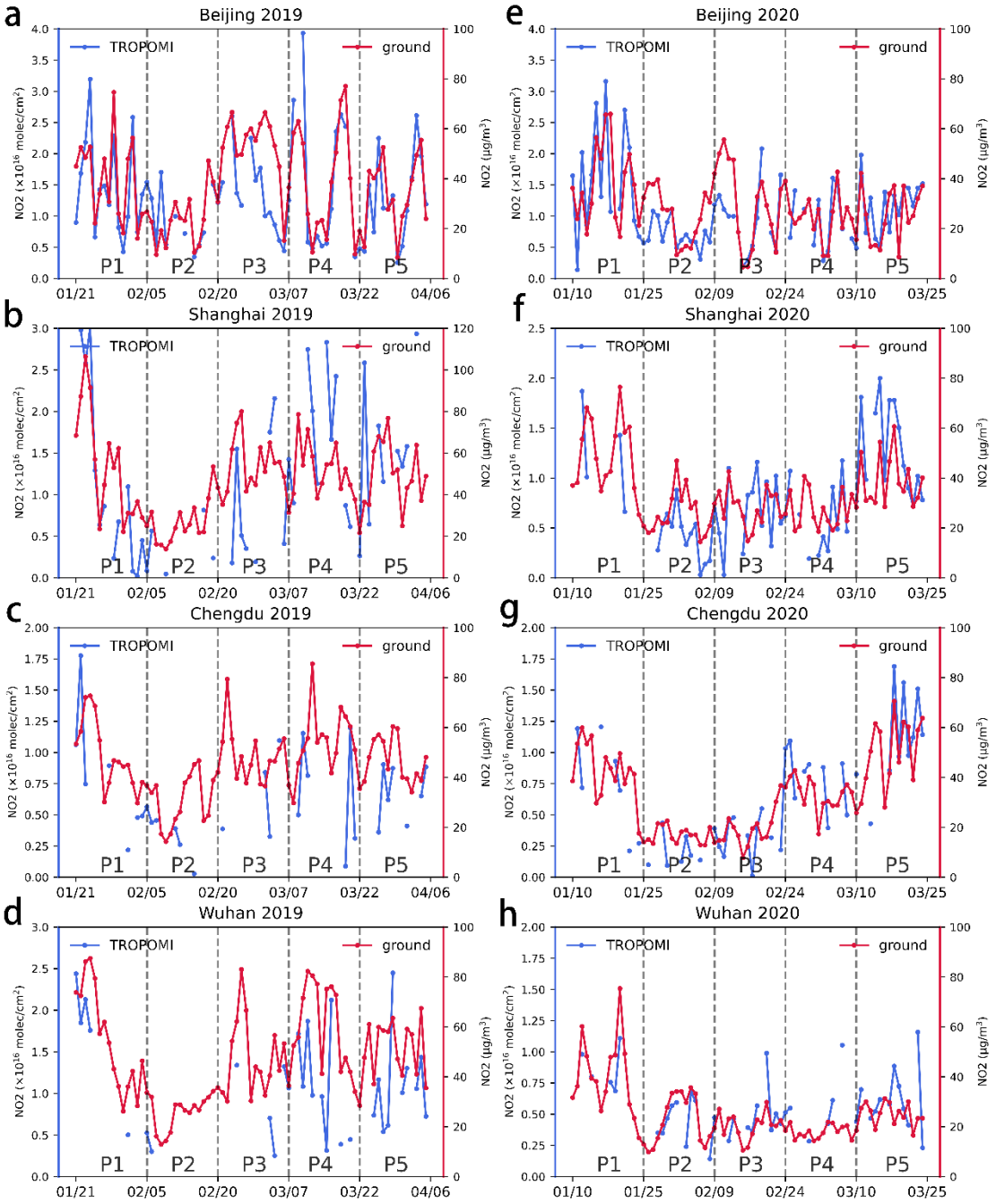


Figure S4. Change in the daily average NO_2 concentration in selected Chinese cities in 2020 compared with 2019, (a–d) 2019, (e–h) 2020.

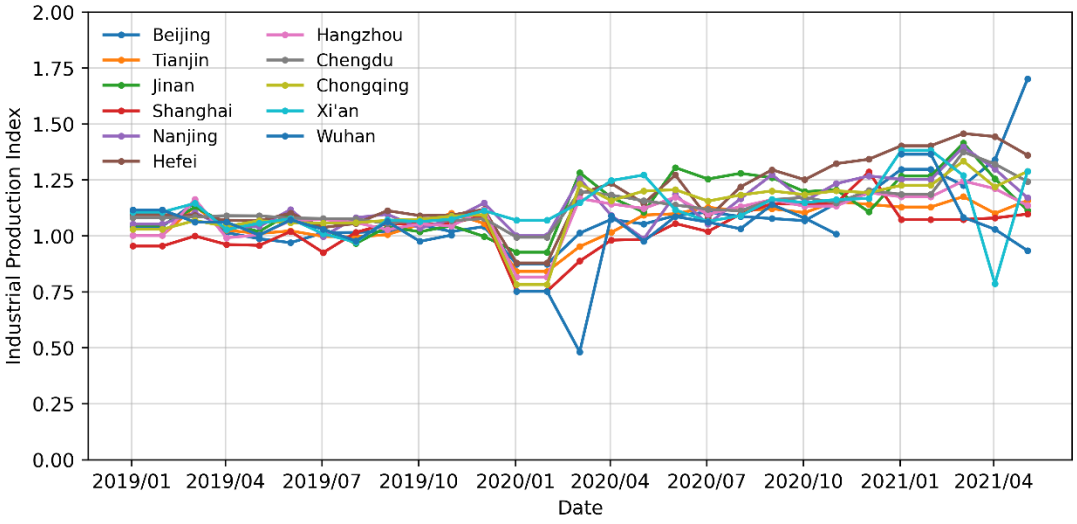


Figure S5. Time series of the above-scale industrial production index in several Chinese cities.

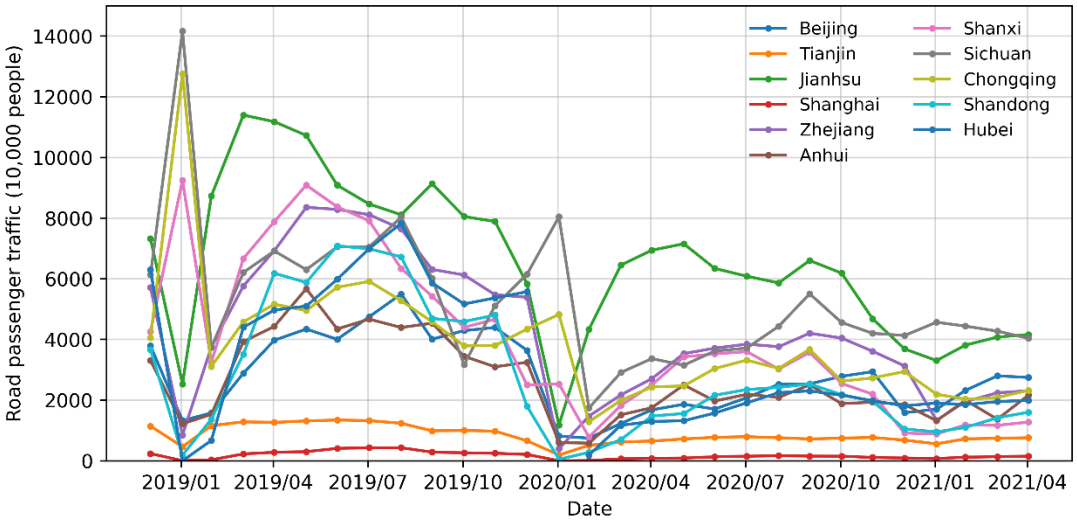


Figure S6. Time series of the road passenger traffic in selected provinces in China.

Supplement Tables

Table S1. Geographical location and number of sites in selected cities in China selected for this study.

City name	Province	Region	Latitude(°)	Longitude(°)	Number of sites
Beijing	Beijing	North China Plain	40.0	116.3	12
Tianjin	Tianjin	North China Plain	39.0	117.1	14
Jinan	ShanDong	North China Plain	36.8	117.0	12
Shanghai	Shanghai	Yangtze River delta	30.0	121.5	10
Nanjing	Jiangsu	Yangtze River delta	32.2	118.9	13
Hefei	Anhui	Yangtze River delta	32.0	117.2	10
Hangzhou	Zhejiang	Yangtze River delta	30.2	120.2	11
Chengdu	Sichaun	Sichuan Basin	30.5	104.0	10
Chongqing	Chongqing	Sichuan Basin	29.5	106.4	16
Wuhan	Hubei	Jianghan Plain	30.5	114.2	11
Xi'an	Shanxi	Guanzhong Basin	34.3	109.0	13

Table S2. Satellite NO_2 TVCD for selected cities in China Percentage decrease by time period in 2020 compared to 2019.

	P1	P2	P3	P4	P5
Beijing	-12.15%	15.14%	23.09%	31.77%	9.84%
Tianjin	-5.03%	14.95%	38.19%	18.51%	5.61%
Jinan	27.37%	30.85%	47.45%	31.26%	21.36%
Shanghai	38.69%	-13.17%	53.76%	60.21%	26.28%
Nanjing	38.23%	0.06%	51.70%	15.04%	-3.04%
Hefei	46.42%		42.20%	2.62%	1.00%
Hangzhou	45.73%		62.92%	25.77%	9.28%
Chengdu	-20.17%	44.51%	55.70%	8.74%	-50.06%
Chongqing	14.18%	47.47%		5.85%	-22.20%
Wuhan	48.12%		42.15%	26.68%	26.77%
Xi'an	-2.75%	19.36%	51.59%	6.31%	-19.70%

Table S3. In-situ observation of NO_2 concentration for selected cities in China Percentage decrease by time period in 2020 compared to 2019.

	P1	P2	P3	P4	P5
Beijing	4.65%	-7.80%	42.53%	36.80%	24.91%
Tianjin	-20.92%	-5.71%	45.71%	22.49%	-0.90%
Jinan	-14.10%	33.10%	69.81%	31.35%	22.82%
Shanghai	8.18%	1.91%	47.39%	47.34%	20.89%
Nanjing	13.81%	21.00%	54.69%	41.99%	10.64%
Hefei	4.51%	9.83%	57.62%	40.09%	13.80%
Hangzhou	14.33%	49.69%	64.20%	31.15%	11.33%
Chengdu	12.41%	45.10%	60.94%	37.78%	-5.97%
Chongqing	11.20%	26.47%	44.00%	43.98%	3.71%
Wuhan	27.39%	12.31%	56.83%	69.62%	51.18%
Xi'an	5.29%	40.24%	47.56%	30.49%	9.94%

Table S4. Satellite NO_2 TVCD for selected cities in China Percentage decrease by time period in 2021 compared to 2019.

	P1	P2	P3	P4	P5
Beijing	29.77%	7.90%	-12.69%	42.25%	24.87%
Tianjin	17.78%	-15.33%	8.80%	15.32%	24.33%
Jinan	37.06%	-3.99%	14.68%	19.34%	36.96%
Shanghai	64.96%	-38.57%	38.58%	10.17%	52.08%
Nanjing	42.35%	-53.37%	14.38%	11.42%	-8.21%
Hefei	44.50%		45.67%	31.48%	17.01%
Hangzhou	34.16%		22.06%	0.16%	2.91%
Chengdu	-10.79%	-37.49%	28.34%	3.46%	-32.32%
Chongqing	10.42%	-47.64%		28.30%	
Wuhan	46.72%		13.43%	25.92%	35.90%
Xi'an	18.62%	-0.88%	13.06%	-29.49%	41.68%

Table S5. In-situ observation of NO_2 concentration for selected cities in China Percentage decrease by time period in 2021 compared to 2019.

	P1	P2	P3	P4	P5
Beijing	26.17%	-10.65%	28.15%	16.84%	4.72%
Tianjin	12.40%	-20.76%	25.98%	1.47%	-21.19%
Jinan	27.07%	29.73%	51.19%	20.41%	11.24%
Shanghai	28.58%	-7.82%	32.08%	17.79%	27.77%
Nanjing	34.99%	27.74%	33.87%	25.42%	27.41%
Hefei	24.18%	3.72%	26.51%	23.20%	25.14%
Hangzhou	28.34%	17.85%	21.02%	9.72%	12.80%
Chengdu	-1.02%	4.57%	15.84%	19.15%	23.04%
Chongqing	4.33%	-20.21%	15.30%	31.54%	27.08%
Wuhan	13.61%	-23.54%	15.53%	28.93%	18.56%
Xi'an	1.05%	-8.43%	15.55%	3.93%	32.04%

References

1. Fayt, C.D.S., I.; Letocart, V.; Merlaud, A.; Pinardi, G.; Van Roozendael, M.; Roozendael, M. . QDOAS Software user manual. *Belg. Inst. Space Aeron. Bruss. Belg.* **2011,7**, 1-117.
2. Zara, M.; Boersma, K.F.; De Smedt, I.; Richter, A.; Peters, E.; van Geffen, J.H.G.M.; Beirle, S.; Wagner, T.; Van Roozendael, M.; Marchenko, S.; et al. Improved slant column density retrieval of nitrogen dioxide and formaldehyde for OMI and GOME-2A from QA4ECV: intercomparison, uncertainty characterisation, and trends. *Atmospheric Measurement Techniques* **2018**, *11*, 4033-4058, doi:10.5194/amt-11-4033-2018.
3. Spurr, R.J.D. VLIDORT: A linearized pseudo-spherical vector discrete ordinate radiative transfer code for forward model and retrieval studies in multilayer multiple scattering media. *J Quant Spectrosc Ra* **2006**, *102*, 316-342, doi:10.1016/j.jqsrt.2006.05.005.
4. Kuhlmann, G.; Lam, Y.F.; Cheung, H.M.; Hartl, A.; Fung, J.C.H.; Chan, P.W.; Wenig, M.O. Development of a custom OMI NO2 data product for evaluating biases in a regional chemistry transport model. *Atmospheric Chemistry and Physics* **2015**, *15*, 5627-5644, doi:10.5194/acp-15-5627-2015.
5. Zhang, C.X.; Liu, C.; Chan, K.L.; Hu, Q.H.; Liu, H.R.; Li, B.; Xing, C.Z.; Tan, W.; Zhou, H.J.; Si, F.Q.; et al. First observation of tropospheric nitrogen dioxide from the Environmental Trace Gases Monitoring Instrument onboard the GaoFen-5 satellite. *Light-Sci Appl* **2020**, *9*.
6. Zhu, Y.Z.; Hu, Q.H.; Gao, M.; Zhao, C.; Zhang, C.X.; Liu, T.; Tian, Y.; Yan, L.; Su, W.J.; Hong, X.H.; et al. Quantifying Contributions of Local Emissions and Regional Transport to NOX in Beijing Using TROPOMI Constrained WRF-Chem Simulation. *Remote Sensing* **2021**, *13*, doi:ARTN 179810.3390/rs13091798.
7. Kuhlmann, G.; Hartl, A.; Cheung, H.M.; Lam, Y.F.; Wenig, M.O. A novel gridding algorithm to create regional trace gas maps from satellite observations. *Atmospheric Measurement Techniques* **2014**, *7*, 451-467, doi:10.5194/amt-7-451-2014.